MATILDITE, ARAMAYOITE, MIARGYRITE[1]

A. R. GRAHAM[2]

Mines Branch, Ottawa, Canada

ABSTRACT

Matildite, aramayoite, and miargyrite are mineral examples of non-isomorphous structures, the atomic arrangements in which are nevertheless closely similar. Triclinic face-centred sub-cells with similar dimensions to the face-centred cubic cells of the high temperature isomorphous series $AgBiS_2$-$AgSbS_2$ can be chosen in all three structures, and are manifest in the galena-like grouping of the powder pattern lines. Long annealing of the metastable artificial members below the inversion temperature induced partial ordering in their disordered structures and gave products with similar powder patterns to those of matildite and aramayoite. New orthorhombic body-centred lattice dimensions, $a = 3.918$, $b = 4.046$, $c = 5.662$ kX are given for matildite; the structural lattice dimensions of aramayoite are refined to Triclinic Pinacoidal-$\bar{1}$, $a = 7.72$, $b = 8.82$, $c = 8.30$ kX, $\alpha = 100°22\frac{1}{2}'$, $\beta = 90°00'$, $\gamma = 103°54'$; and indexed powder patterns are given for all three minerals and three of the annealed artificial products.

A series of seven pyrosynthetic compounds covering the full range $AgBiS_2$-$AgSbS_2$ gave a practically constant face-centred cubic pattern of the galena type. The three known minerals in this series, matildite $AgBiS_2$, aramayoite $Ag(Sb,Bi)S_2$ with $Sb:Bi = 5:1$, and miargyrite $AgSbS_2$ are orthorhombic, triclinic, and monoclinic, respectively, with complex x-ray powder patterns in which groups of lines can be recognized in place of single lines in the galena-type patterns of the pyrosynthetic products. From this it is apparent that there are high temperature (cubic) and low temperature (non-cubic) forms throughout the series. Pyrosynthesis produces the high temperature (α) forms which on rapid cooling persist as metastable compounds at room temperature. From the fact that these α-modifications give the galena type of pattern, it is evident that their unit cells contain $Ag_2(Bi,Sb)_2S_4$, with Ag, Bi, and Sb acting as equivalent metallic atoms in a rock-salt arrangement, M_4S_4. In the corresponding minerals representing the low temperature β-modifications the modified galena type of pattern shows that these less symmetrical structures represent some modification of the rock-salt arrangement by atoms of different kinds assuming special positions in larger cells with lower symmetries. This is entirely in keeping with the known disorder-order relations in many metallic compounds.

It was therefore decided to attempt to induce the α-β inversion in artificial compounds of the series, and also to correlate the crystallography

---

[1] Published by permission of the Director-General of Scientific Services, Department of Mines and Technical Surveys, Ottawa.

[2] Mineragrapher, Department of Mines and Technical Surveys. Ottawa.

of the three minerals which superficially show little relation to their common cubic high temperature prototype.

Matildite $AgBiS_2$ is commonly more or less intergrown with galena ("schapbachite," "plenargyrite"). Ramdohr (1938) studied these intergrowths in detail with the aid of x-ray powder photographs made with a heating camera. Below about 210° C. mineral samples gave mixed patterns of matildite (β-$AgBiS_2$) and galena; above this temperature the pure galena type of pattern was obtained indicating inversion of matildite to α-$AgBiS_2$ which is isostructural with galena and makes a homogeneous solid solution with the lead compound. For α-$AgBiS_2$ Ramdohr gives $a = 5.64$ A; β-$AgBiS_2$ was found to be orthorhombic with $a = 8.14$, $b = 7.87$, $c = 5.69$ A, from the powder patterns.

Aramayoite $Ag(Sb,Bi)S_2$ (Spencer, 1926) was studied with the Bragg x-ray spectrometer by Yardley—now Mrs. K. Lonsdale—(1926), who obtained a pseudo-cubic triclinic cell with $a = 5.67$, $b = 5.69$, $c = 5.623$ A, $\alpha = 86°55'$, $\beta = 90°53'$, $\gamma = 93°18'$. From the intensities it appeared that the heavy atoms, Ag, (Sb,Bi), must make a face-centred lattice while the light S atoms might be placed as in a rock-salt type of structure. On well developed crystals of aramayoite from the original locality Berman & Wolfe (1939) obtained entirely different triclinic cell dimensions: $a = 7.76$, $b = 8.79$, $c = 8.34$ kX, $\alpha = 100°22'$, $\beta = 90°00'$, $\gamma = 103°54'$. This cell conforms to the morphology but shows no immediate relation to the pseudo-cubic cell of Yardley.

The structure of miargyrite was determined by Hofmann (1938) using the Weissenberg method. The distribution of the strong diffractions on the photographs showed a pseudo-cubic face-centred arrangement of the heavy atoms which was recognized as similar to that in the aramayoite structure given by Yardley, and to the probable structure of matildite. Hofmann obtained monoclinic lattice dimensions, $a = 13.17$, $b = 4.39$, $c = 12.83$ kX, $\beta = 98°37\frac{1}{2}'$.

MATILDITE

As the lattice dimensions of matildite given in Ramdohr (1938) had been obtained from powder patterns alone, it was considered desirable to try to prepare single crystals of β-$AgBiS_2$ on which to check the cell elements. Accordingly, crystals giving the face-centred cubic powder pattern of α-$AgBiS_2$ were hydrosynthesized in a pressure bomb from alkaline sodium sulphide solution of appropriate constituents, after the method developed by Dr. F. G. Smith of the University of Toronto. Several dozen of these, ranging in size from 0.1 to 0.5 mm., were picked under the microscope from their locations scattered freely throughout blades and felted masses of crystalline bismuth sulphide, or attached

loosely by an edge or apex to masses of anhedral silver sulphide. Microchemical tests showed silver, bismuth, and sulphur. The Talmadge hardness was $B+$, estimated by needle scratch on an octahedral face. Careful crushing yielded a black powder assuming dark reddish tones on finer pulverization, while rubbing under the pestle revealed some malleability and produced thin gray flakes. Powder photographs on crushed crystals showed a cubic face-centred pattern giving a cell-edge which compares closely with that given by Ramdohr (1938) for matildite above 215° C.; a check on the composition of the hydrosynthetic material was obtained by an identical powder photograph from a homogeneous air-quenched fusion product of composition $AgBiS_2$.

α-$AgBiS_2$ (pyrosynthetic)	$a = 5.636$ kX A.R.G.
α-$AgBiS_2$ (hydrosynthetic)	$a = 5.635$ kX A.R.G.
α-$AgBiS_2$ (matildite at 215° C.)	$a = 5.64$ kX Ramdohr (1938)

Several hydrosynthetic crystals and a portion of the fusion product of the same composition were sealed in separate evacuated pyrex tubes together with a few milligrams of sulphur to combine with residual oxygen. The tubes were heated in a constant temperature oven at 180° C. for nine days, then air-quenched. Part of the fusion product was mounted and polished for optical examination. Weak anisotropism and accentuated grain boundaries were seen upon comparison with the original isotropic material. Etch-tests upon the annealed portion were almost identical with those given by Ramdohr (1938) for matildite, but less rapid action was observed with 1:1 HNO_3.

Powder photographs of the annealed fusion product and of annealed crystals showed each line of the face-centred cubic pattern divided into two or more separate lines, indicating a change to lower symmetry, more complete in the case of the fusion product. In the pattern of the latter material, several of the strong lines of Ag_2S appeared after annealing. Re-examination of the polished section at high magnification revealed tiny areas of Ag_2S and Bi_2S_3, in approximately equal amounts, less than 1% of the whole, included in grains of the main phase to one side of the section. Fortuitous inclusion of Ag_2S in the annealed x-ray powder sample had apparently occurred in an amount large enough to suggest segregation of two phases during annealing, although the amount of uncombined Ag_2S present by visual comparison was insufficient to affect to any noticeable degree the composition of the main phase. Incomplete reaction of the components during fusion is the most likely explanation.

An individual annealed crystal rotated on a random axis in the powder camera gave a pattern which indicated almost complete inversion, and whose spots superimposed perfectly upon all but the Ag_2S lines of the powder pattern of the annealed fusion product. Comparison of the meas-

urements with measurements on a powder pattern of natural matildite and galena from Schapbach, Baden, by R. M. Thompson, showed substantial agreement in the spacings and intensities of lines after elimination of the galena lines from the pattern of the mineral. Thus α-AgBiS$_2$, cubic in symmetry, had inverted to a β-form of lower symmetry identical with matildite.

The same crystal which had yielded the β-AgBiS$_2$ powder pattern was oriented to rotate about the apparent four-fold symmetry axis. The signals on the optical goniometer were weaker and more diffuse than before inversion, but the measured angles were still within a few minutes of those of the octahedron. A rotation photograph about this axis superimposed upon one taken before inversion showed retention of cubic diffractions, much diminished in intensity, and the appearance of extra diffractions from inverted portions of the crystal. Layer lines were paired, and two choices of period were possible, one 5.662 kX; the other 5.50 kX calculated from the spacings of each pair of ($hk1$) and ($hk2$) layer lines registered on the photograph.

Weissenberg zero and first layer photographs about this same axis were moderately successful, but a twelve hour exposure failed to resolve weak second-layer diffractions. The zero layer diffractions were characteristic of a body-centred orthorhombic lattice twinned on (110). Extra diffractions defining the twinned orthorhombic lattice appeared on the ($h00$) and ($0k0$) rows closely bracketing spots which superimposed perfectly on those of the zero layer photograph about the same axis, a principal cubic axis before inversion. The cubic diffractions were assumed to belong to an uninverted portion of the crystal. A schematic representation of the zero and first layers of the twinned reciprocal lattice appears in Fig. 1 with the cubic diffractions omitted. In the terminology of Friedel the obliquity of the twin is 1°50′.

From the Weissenberg and rotation photographs elements were calculated which agree poorly with those given for matildite by Ramdohr (1938), after halving and interchanging his a and b periods.

Matildite (Ramdohr)	β-AgBiS$_2$ (A.R.G.)
$b/2 = 3.935$ kX	$a = 3.918$ kX
$a/2 = 4.07$	$b = 4.046$
$c = 5.69$	$c = 5.662$

Table 1 contains the powder pattern of artificial β-AgBiS$_2$ and that of material labelled matildite from Schapbach, (galena lines eliminated) indexed using the elements obtained from the inverted hydrosynthetic crystals and also according to the pseudo-cubic face-centred setting analogous to the high temperature lattice. Better agreement was obtained between measured and calculated spacings than with the elements quoted in Ramdohr (1938).

The relation of the body centred orthorhombic unit cell of β-AgBiS$_2$ (matildite) to the face-centred cubic (now pseudo-cubic) cell of α-AgBiS$_2$ is shown in Figure 2a. One might infer that the inversion α to β was accompanied by a segregation of the (Ag, Bi) atoms, which are equivalent
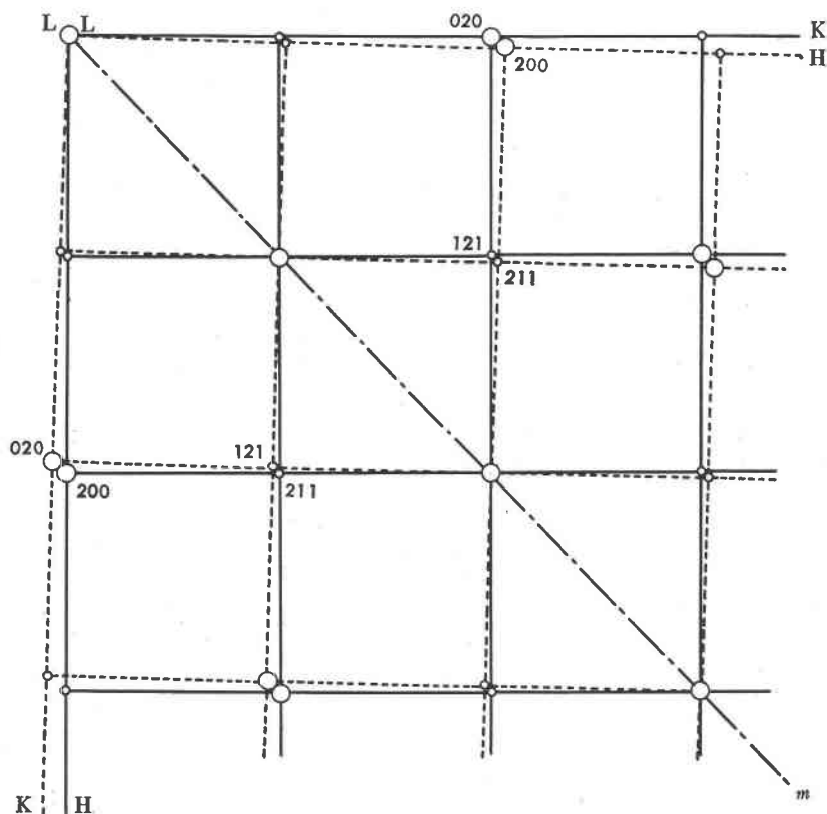

Fig. 1.—Schematic reciprocal lattice plot from 0- and 1-layer Weissenberg photographs of twinned annealed AgBiS$_2$ crystal. Large circles are 0-layer diffractions, small circles 1-layer diffractions. Solid and dotted lines define lattices of individuals twinned on (110). Chained line is the trace of the twin plane m(110).

in the cubic structure, into Ag atoms, say, at the origin of the orthorhombic cell and Bi at the body-centre. However, the fact that β-AgBiS$_2$ still gives the systematically missing spectra of the body-centred lattice shows that such segregation of Ag and Bi cannot have proceeded very far.

ARAMAYOITE AND MIARGYRITE

The unit cell of aramayoite was checked by Professor Peacock from a consideration of the results of Berman & Wolfe and those of Yardley to-

TABLE 1. COMPARISON OF MATILDITE AND β-AgBiS$_2$ POWDER PATTERNS

Orthorhombic, I; $a=3.918$, $b=4.046$, $c=5.662$ kX; $Z=1$

1		2		3	4	5
I(Cu)	d(meas.)	I(Cu)	d(meas.)	(hkl)	(hkl)	d(calc.)
6	3.32kX	8	3.29 kX	(111)	(011)	3.292 kX
2	3.18	1	3.16	(1$\bar{1}$1)	(101)	3.222
10	2.83	10	2.82	$\begin{cases}(002)\\(200)\end{cases}$	(002) (110)	2.831 2.814
3	2.03	6	2.03	(220)	(020)	2.023
5	1.963	5	1.967	(2$\bar{2}$0)	(200)	1.960
3	1.711	3	1.708	$\begin{cases}(311)\\(113)\end{cases}$	(121) (013)	1.713 1.710
$\frac{1}{2}$	1.670	$\frac{1}{2}$	1.670	(3$\bar{1}$1)	(211)	1.683
1	1.648	$\frac{1}{2}$	1.648	(222)	(022)	1.646
2	1.583	$\frac{1}{2}$	1.586	(2$\bar{2}$2)	(202)	1.611
3	1.396	1	1.411	$\begin{cases}(004)\\(400)\end{cases}$	(004) (220)	1.416 1.407
4	1.322	1	1.316	(331)	(031)	1.312
$\frac{1}{2}$	1.285	1	1.282	(420)	(130)	1.275
2	1.249	1	1.247	(4$\bar{2}$0)	(310)	1.243
—	—	$\frac{1}{2}$	1.167	(422)	(132)	1.163
$\frac{1}{2}$	1.160	$\frac{1}{2}$	1.158	(224)	(024)	1.160
—	—	$\frac{1}{2}$	1.072	$\begin{cases}(5\bar{1}1)\\(333)\end{cases}$	(321) (303)	1.077 1.074
—	—	$\frac{1}{2}$	0.968	(531)	(141)	0.965
—	—	$\frac{1}{2}$	0.884	(6$\bar{2}$0)	(420)	0.882

1. Measurements and observed intensities on material from Schapbach, Baden, Germany, with galena lines removed; after R. M. Thompson, University of Toronto (unpublished data).

2. Measurements and observed intensities from annealed artificial crystals, by A. R. Graham (Ag$_2$S lines removed).

3. Indices according to pseudo-cubic face-centered lattice.

4. Indices in structural setting.

5. Spacings calculated from structural elements.

gether with some new measurements on type material. The adopted cell elements differ only slightly from those of Berman & Wolfe (Table 2) and the correctness of the new values is indicated by the indexed powder pattern (Table 4). The transformation of Yardley's setting to that of Berman & Wolfe was also verified.

TABLE 2. ARAMAYOITE: CELL DIMENSIONS

	1	2	3	4
a	7.72 kX	—	(7.76) kX	—
b	8.82	—	(8.79)	
c	8.30	8.34 kX	(8.34)	—
$d(100)$	7.49	7.52	7.50	$6d(33\bar{1})$ 7.56 kX
$d(010)$	8.42	8.41	8.43	$d(001)$ 8.415
$d(001)$	8.16	—	8.16	$6d(\bar{3}31)$ 8.13
α	$100°22\frac{1}{2}'$	—	$100°22'$	—
β	$90°00'$	$90°00'$	$90°00'$	—
γ	$103°54'$	—	$103°54'$	—

1. Adopted by Peacock as best representing the available measurements.
2. Measured by Peacock.
3. Given by Berman & Wolfe (1939); a, b, c, were computed in a manner which cannot now be ascertained; α, β, γ, are morphological values.
4. Spacings observed by Yardley (1926) on the ionization spectrometer; it is assumed that Yardley's planes ($\bar{3}1\bar{3}$) are in fact ($\bar{3}31$).

Hofmann's (1938) unit cell of miargyrite was retained and the relation to the pseudo-cubic sublattice was worked out with the help of information in his published work.

For convenient comparison, the cell dimensions of the pseudo-cubic face-centred sub-lattices present in all three minerals were calculated using the general formulae for lattice periods and angles. The transformation formulae involved in the calculation of cell elements are as follows:

Matildite:
  Graham to Pseudo-cubic $110/\bar{1}10/001$
  Pseudo-cubic to Graham $\frac{1}{2}\frac{1}{2}0/\frac{1}{2}\frac{1}{2}0/001$

Aramayoite:
  Berman & Wolfe to Yardley $\frac{1}{2}0\frac{1}{2}/\frac{1}{2}0\frac{1}{2}/\frac{1}{6}\frac{2}{3}\frac{1}{6}$
  Yardley to Berman & White $\bar{1}10/\frac{1}{2}0\frac{3}{2}/\bar{1}10$

Miargyrite:
  Hofmann to Pseudo-cubic $\frac{1}{8}1\frac{1}{4}/\frac{1}{8}1\frac{1}{4}/\frac{3}{8}0\frac{1}{4}$
  Pseudo-cubic to Hofmann $1\bar{1}2/\frac{1}{2}\frac{1}{2}0/\frac{3}{2}\frac{3}{2}1$

The dimensions of the sub-lattices given in Table 3 show a striking similarity which is not immediately evident in the lattices established by

x-ray and optical goniometrical studies. Figs. 2a, b, c show the relation-ship of the sub-lattices to the lattices in structural settings by means of individual cells viewed in the conventional manner. The pseudo-cubic face-centred cell of β-AgBiS$_2$ is actually twice as large as the unit cell but for the sake of clarity, is still called a sub-lattice by analogy with those of the other two minerals. In the diagrams, structural lattice points are filled circles; sub-lattice points are left open. In all the structures, all these points must be occupied by heavy atoms (Hofmann, 1938).

TABLE 3. COMPARISON OF LATTICE DIMENSIONS (kX)

	Matildite		Aramayoite		Miargyrite	
	Struct. Lattice	Ps-cub. Sub. Latt.	Struct. Lattice	Ps-cub. Sub. Latt.	Struct. Lattice	Ps-cub. Sub. Latt.
a	3.918	5.632	7.72	5.67	13.17	5.818
b	4.046	5.632	8.82	5.67	4.39	5.818
c	5.662	5.662	8.30	5.62	12.83	5.471
α	90°00′	90°00′	100°22½′	86°42′	90°00′	88°58′
β	90°00′	90°00′	90°00′	91°33′	98°37½′	91°02′
γ	90°00′	88°10′	103°54′	94°8½′	90°00′	82°02′
V	89.76	179.5	539.1	179.9	733.4	183.3 kX³
Z	1	2	6	2	8	2

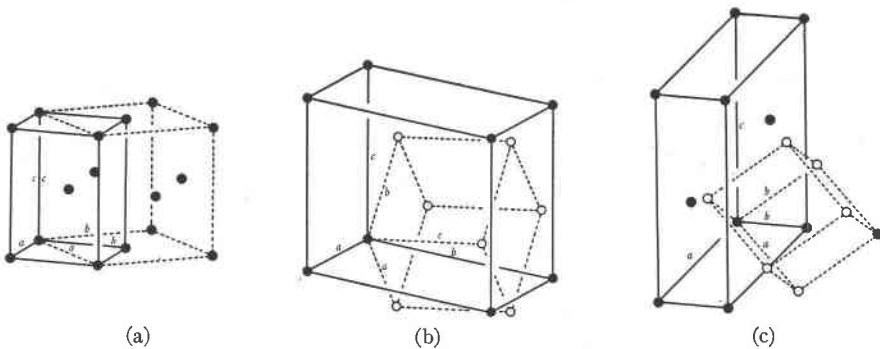(a)   (b)   (c)

FIG. 2.—Structural unit cells (solid lines) and pseudo-cubic sub-lattices (dotted lines) of (a) matildite, (b) aramayoite, (c) miargyrite. Filled circles are structural lattice points; open circles are sub-lattice points. Face-centre points of sub-lattice omitted for clarity in (b) and (c).

It is apparent that an ordering process during inversion (cooling) which involves a slight adjustment of bond length as well as the lowering of symmetry by assumption of special positions by atoms of particular elements, could satisfy the observed facts concerning the lattices of all

TABLE 4. ARAMAYOITE-Ag(Sb,Bi)S$_2$: X-RAY POWDER PATTERN
Triclinic, $\bar{1}$; $a = 7.72$, $b = 8.82$, $c = 8.30$ kX;
$\alpha = 100°22\frac{1}{2}'$, $\beta = 90°00'$, $\gamma = 103°54'$; $Z = 6$

I(obs.)	θ(Cu)	d(meas.)	(hkl)*	(hkl)	d(calc.)
2	12.95°	3.43 kX	($\bar{1}$11)	(012)	3.428 kX
4	13.85	3.21	{ ($1\bar{1}1$)	($02\bar{2}$)	3.244
			(111)	($\bar{2}20$)	3.213
1	14.15	3.15	($\bar{1}\bar{1}1$)	(210)	3.146
10	15.90	2.806	{ (200)	($\bar{2}1\bar{2}$)	2.826
			(020)	($\bar{2}0\bar{2}$)	2.822
			(002)	(030)	2.804
2	22.05	2.048	(022)	($\bar{2}3\bar{2}$)	2.047
$\frac{1}{2}$	22.45	2.015	($\bar{2}02$)	(222)	2.014
$\frac{1}{2}$	23.00	1.967	(202)	($\bar{2}4\bar{2}$)	1.968
3	23.35	1.940	{ ($0\bar{2}2$)	($23\bar{2}$)	1.936
			(220)	($\bar{4}10$)	1.930
$\frac{1}{2}$	25.95	1.757	{ ($\bar{1}31$)	($\bar{2}14$)	1.767
			($\bar{3}11$)	(204)	1.757
1	26.25	1.738	($\bar{1}13$)	(042)	1.742
2	26.80	1.705	{ ($3\bar{1}1$)	($\bar{2}3\bar{4}$)	1.716
			($\bar{2}22$)	(024)	1.714
			($\bar{1}31$)	($22\bar{4}$)	1.704
			(113)	($\bar{2}50$)	1.698
			(131)	($\bar{4}22$)	1.691
1	27.45	1.668	{ ($\bar{3}\bar{1}1$)	(402)	1.673
			(311)	($\bar{4}3\bar{2}$)	1.669
			($1\bar{1}3$)	($05\bar{2}$)	1.668
			($\bar{1}\bar{1}3$)	(240)	1.668
1	28.45	1.614	{ ($2\bar{2}2$)	($04\bar{4}$)	1.622
			(222)	($\bar{4}40$)	1.607
$\frac{1}{2}$	29.15	1.578	($\bar{2}22$)	(420)	1.573
$\frac{1}{2}$	32.95	1.413	{ (400)	($\bar{4}2\bar{4}$)	1.413
			(040)	($\bar{4}0\bar{4}$)	1.411
2	33.25	1.402	(004)	(060)	1.402

I(obs)	θ(Cu)	d(meas.)	I(obs)	θ(Cu)	d(meas.)	I(obs)	θ(Cu)	d(meas.)
$\frac{1}{2}$	34.85°	1.345 kX	$\frac{1}{2}$	37.25°	1.270 kX	$\frac{1}{2}$	42.65°	1.135 kX
$\frac{1}{2}$	36.45	1.294	$\frac{1}{2}$	38.35	1.239	$\frac{1}{2}$	45.05	1.086
$\frac{1}{2}$	36.80	1.283	$\frac{1}{2}$	41.75	1.154	$\frac{1}{2}$	45.85	1.071

* Pseudo-cubic face-centered sub-lattice indices.

TABLE 5. MIARGYRITE-AgSbS$_2$: X-RAY POWDER PATTERN

Monoclinic, $A2/m$; $a=13.17$, $b=4.39$, $c=12.83$ kX; $\beta=98°37\frac{1}{2}'$; $Z=8$

I(obs.)	θ(Cu)	d(meas.)	(hkl)*	(hkl)	d(calc.)
9	12.90°	3.443 kX	(111)	(211)	3.423 kX
2	14.00	3.178	($\bar{1}$11)	(004)	3.171
2	14.40	3.091	(1$\bar{1}$1)	(40$\bar{2}$)	3.091
10	15.50	2.877	(200)	(21$\bar{3}$)	2.881
8	16.30	2.739	(002)	(402)	2.734
$\frac{1}{2}$	20.40	2.205	(220)	(020)	2.195
4	22.55	2.005	(022)	(215)	2.004
4	23.10	1.963	(0$\bar{2}$2)	(6$\bar{1}\bar{1}$)	1.963
3	23.75	1.909	(2$\bar{2}$0)	(40$\bar{6}$)	1.909
1	25.30	1.799	(131)	(024)	1.805
2	25.40	1.792	(311)	(42$\bar{2}$)	1.790
$\frac{1}{2}$	26.65	1.714	(222)	(422)	1.712
3	27.20	1.682	$\begin{cases}(113)\\(\bar{1}31)\end{cases}$	(613) / ($\bar{2}$17)	1.684 / 1.679
1	27.65	1.657	$\begin{cases}(\bar{1}13)\\(1\bar{3}1)\end{cases}$	(406) / (6$\bar{1}\bar{5}$)	1.663 / 1.655
$\frac{1}{2}$	28.25	1.624	(1$\bar{1}$3)	(800)	1.628
2	29.00	1.586	($\bar{2}$22)	(008)	1.585
2	29.85	1.544	(2$\bar{2}$2)	(80$\bar{4}$)	1.545
$\frac{1}{2}$	31.10	1.488	—	—	—
$\frac{1}{2}$	32.15	1.445	(400)	(42$\bar{6}$)	1.440
$\frac{1}{2}$	32.90	1.415	(331)	(231)	1.414
1	34.20	1.368	(004)	(804)	1.368

I(obs)	θ(Cu)	d(meas.)	I(obs)	θ(Cu)	d(meas.)	I(obs)	θ(Cu)	d(meas.)
$\frac{1}{2}$	35.40°	1.327 kX	$\frac{1}{2}$	43.05°	1.126 kX	1	53.60°	0.955 kX
$\frac{1}{2}$	35.90	1.311	$\frac{1}{2}$	44.05	1.106	$\frac{1}{2}$	56.30	0.924
$\frac{1}{2}$	36.90	1.280	$\frac{1}{2}$	44.35	1.100	$\frac{1}{2}$	58.40	0.902
$\frac{1}{2}$	37.50	1.263	$\frac{1}{2}$	45.10	1.085	$\frac{1}{2}$	59.10	0.896
2	38.10	1.246	$\frac{1}{2}$	45.60	1.076	$\frac{1}{2}$	61.10	0.878
$\frac{1}{2}$	38.70	1.229	$\frac{1}{2}$	46.35	1.062	$\frac{1}{2}$	62.40	0.867
$\frac{1}{2}$	38.90	1.224	$\frac{1}{2}$	50.05	1.003	$\frac{1}{2}$	65.80	0.843
$\frac{1}{2}$	41.40	1.162	$\frac{1}{2}$	51.15	0.987	$\frac{1}{2}$	69.15	0.823
$\frac{1}{2}$	42.25	1.144	$\frac{1}{2}$	52.00	0.975	$\frac{1}{2}$	75.15	0.795

Elements after Hofmann (1938).

* Pseudo-cubic face-centred sub-lattice indices. Measurements by Graham on U. of T. Spec. R569: Miargyrite Braunsdorf, Saxony. Indexed by transformation from pseudo-cubic face-centred sub-cell.

three compounds. As would be expected, the miargyrite sublattice shows the greatest aberrance from a high-symmetry disordered lattice: the smaller radius of the Sb atom compared to those of Ag and Bi would produce a greater distortion.

For the identification of aramayoite and miargyrite their complex x-ray powder patterns were indexed in a practical way suggested by Professor Peacock. This is based on the assumption that the powder diffractions would probably all be due to the heavy atoms, which are situated at the points of the face-centred pseudo-cubic sub-lattices; and that therefore it would suffice to calculate the spacings of all sets of planes, in the desired range, corresponding to indices conforming to the F-condition in the sub-lattice. This assumption proved to be justified as seen in the indexed patterns (Tables 4 and 5).

INVERSION EXPERIMENTS IN THE SYSTEM $AgBiS_2$-$AgSbS_2$

The successful inversion of the metastable α-$AgBiS_2$ led to an examination of the results of annealing fusion products throughout the system $AgBiS_2$-$AgSbS_2$. Six further fusions including four wtih purposely irrational atomic ratios of Bi to Sb, were carried out in evacuated tubes. The quenched products were examined in polished section and by x-ray powder photographs. All appeared entirely homogenous and gave face-centred cubic powder patterns indicating disordered structures metastable at normal temperatures. The compositions and measured cell-edges are given in Table 6. The cell-edges were calculated from back reflections

TABLE 6. COMPOSITIONS AND CELL-EDGES OF FUSIONS

Fusion	Composition	Cell-edge
A	$AgBiS_2$	5.636 kX
B	$Ag_{10}Bi_9Sb_1S_{20}$	5.640
C	$Ag_{10}Bi_7Sb_3S_{20}$	5.641
D	$Ag_2Bi_1Sb_1S_4$	5.645
E	$Ag_{10}Bi_3Sb_7S_{20}$	5.642
F	$Ag_{10}Bi_1Sb_9S_{20}$	5.636
G	$AgSbS_2$	5.642

from the planes (046), (155) (117), and (444). The adjustment method employed is considered to have reduced the probable error to $\pm$ .003 kX. The fact that the cube-edge is practically constant throughout the series indicates that the large Ag atom in some way controls the lattice parameters in the disordered high temperature structures.

Slow cooling of the fusions over periods up to a few hours in length, had little or no effect on the powder patterns, so the same annealing treat-

ment as with $AgBiS_2$ was attempted upon each of the six new fusions, B to G. Fusions B and F inverted nearly completely after annealing at 180° C. for eight days, while the rest remained either unchanged or showed only slight diffusion of the powder lines indicating some tendency toward inversion. Further treatment at 200° C. for nine days produced definite changes in D and E. Fusions C and G remained unchanged after annealing at 180°, 200°, 210°, 215° C., for periods up to five weeks in duration. After the last annealing experiment attempted, fusion G gave the cubic powder pattern with faint additional extraneous lines which were not obviously related to those of miargyrite or to any of the other low temperature patterns.

Table 7 presents the measured spacings in kX units and the observed intensities of the powder patterns from inverted products, together with portions of the patterns of α-$AgBiS_2$, aramayoite and miargyrite, indexed according to the pseudo-cubic face-centered setting. It will be seen that the inverted product E gives a powder pattern closely comparable to that of aramayoite. An inversion product comparable to miargyrite was not obtained.

CONCLUSIONS

The successfully annealed fusion products in the system $AgBiS_2$-$AgSbS_2$ possess pseudo-cubic sub-lattices closely related to one another and to those possessed by the minerals matildite and aramayoite. These sub-lattices are descended from those of the face-centred cubic high temperature forms, which are truly isomorphous and have disordered structures.

True isomorphism cannot be held to exist in the low temperature forms, even although the arrangement of heavy atoms in the structures is much the same, for the ordering process initiated and accelerated by annealing destroys strict isomorphism by unequal shifts in atomic positions according to the availability of Bi or Sb atoms. Consequently, different structures are possible, although the basic structures differ but slightly.

Possibly a number of structures could be produced during the ordering process in a single compound of this type by annealing within appropriate temperature limits for periods sufficient to permit maximum ordering. In nature, extremely slow cooling from temperature of crystallization may be regarded as the optimum condition for the ordering process to proceed to completion during the fall of the temperature level to normal. We should expect changes to have taken place in the symmetry of some minerals which are irreproducible in the laboratory simply from lack of time.

The crystal habits of aramayoite and miargyrite are in complete harmony with their crystal lattices and show no cubic pseudo-symmetry.

TABLE 7. COMPARISON OF MEASURED SPACINGS OF ANNEALED FUSIONS B AND E
α-AgBiS$_2$, β-AgBiS$_2$, ARAMAYOITE, MIARGYRITE IN kX UNITS

α-AgBiS$_2$ I	d	hkl	β-AgBiS$_2$ I	d	hkl	B I	d	E I	d	Aramayoite I	d	hkl	Miargyrite I	d	hkl
								1	3.39	2	3.43	$\bar{1}11$	9	3.44	111
7	3.23	111	8	3.29	111	1	3.28	6	3.22	4	3.21	$\begin{cases}1\bar{1}1\\111\end{cases}$	2	3.18	$\bar{1}11$
			1	3.16	$1\bar{1}1$	10	3.19								
						½	3.16			1	3.15	$\bar{1}\bar{1}1$	2	3.09	$1\bar{1}1$
10	2.81	002	10	2.82	$\begin{cases}002\\200\end{cases}$	6	2.84	10	2.81	10	2.81	$\begin{cases}200\\020\\002\end{cases}$	10	2.88	200
						6	2.75						8	2.74	002
						2	2.72								
8	1.98	022	3	2.03	220	½	2.03	2	2.05	2	2.05	022	½	2.21	220
								1	2.02	½	2.02	$\bar{2}02$	4	2.01	022
			5	1.97	$2\bar{2}0$	5	1.98			½	1.97	202	4	1.96	$0\bar{2}2$
						3	1.93	3	1.94	3	1.94	$\begin{cases}0\bar{2}\bar{2}\\220\end{cases}$	3	1.91	$2\bar{2}0$
								½	1.90				½	1.80	131
								½	1.76	½	1.76	$\begin{cases}\bar{1}31\\\bar{3}11\end{cases}$	1	1.79	311
4	1.69	113				2	1.72	1	1.75	1	1.74	$\bar{1}13$			
			3	1.71	$\begin{cases}311\\113\end{cases}$	½	1.70	5	1.71	2	1.71	$\begin{cases}\bar{3}11\\\bar{2}22\\1\bar{3}1\\113\\131\end{cases}$	½	1.71	222
			$\bar{1}$	1.67	$3\bar{1}1$	1	1.67	2	1.68	1	1.67	$\begin{cases}\bar{3}11\\311\\1\bar{1}3\\\bar{1}13\end{cases}$	3	1.68	$\begin{cases}113\\\bar{1}31\end{cases}$
													1	1.66	$\begin{cases}131\\\bar{1}13\end{cases}$
2	1.63	222	1	1.65	222	1	1.65	1	1.62	1	1.61	$\begin{cases}2\bar{2}2\\222\end{cases}$	½	1.62	$1\bar{1}3$
													2	1.54	$\bar{2}22$
			½	1.59	$2\bar{2}\bar{2}$	2	1.61			½	1.58	$\bar{2}\bar{2}2$	2	1.54	$\bar{2}22$
								½	1.52				½	1.49	—
1	1.41	004	1	1.41	$\begin{cases}004\\400\end{cases}$	½	1.43	3	1.41	½	1.41	$\begin{cases}400\\040\end{cases}$	½	1.45	400
						½	1.38						½	1.42	331
										2	1.40	004	1	1.37	004

B I	d	E I	d	E I	d	E I	d
½	1.355	½	1.344	½	1.269	½	1.093
½	1.322	½	1.330	½	1.235	½	1.074
½	1.292	½	1.314	½	1.191	½	0.989
1	1.228	½	1.289	½	1.134	½	0.970
½	1.073	½	1.280				
½	0.983						

From this it is almost certain that these minerals crystallized below the inversion temperatures like acanthite and that they are not paramorphs of the corresponding high temperature cubic phases (like argentite).

REFERENCES

BÉLAND, R. (1948): Synthesis of some sulpharsenites of silver in alkali sulphide solutions, *Econ. Geol.*, **43**, 119–132.

BERMAN, H., & WOLFE, C. W. (1939): Crystallography of aramayoite, *Min. Mag.*, **21**, 163–168.

FRIEDEL, G. (1926): *Leçons de crystallographie*, Berger-Levrault, Paris.

HOFMANN, W. (1938): Die Struktur von Miargyrit $AgSbS_2$, *Sitzungsber. Preuss. Akad. Wiss. Phys., Math. Kl.*, VI. 111–119.

RAMDOHR, P. (1938): Über Schapbachit, Matildit und den Silber- und Wismutgehalt mancher Bleiglanze, *Sitzungsber. Preuss. Akad. Wiss. Phys. Math. Kl.*, VI, 71–91.

ROBINSON, S. C. (1948): Synthesis of lead sulphantimonites, *Econ. Geol.* **43**, 293–312.

SMITH, F. G. (1947): Transport and deposition of the non-sulphide vein minerals. II Cassiterite, *Econ. Geol.* **42**, 251–264.

SPENCER, L. S. (1926): Aramayoite, a new mineral from Bolivia, *Min. Mag.*, **21**, 156–162.

YARDLEY, K. (1926): X-ray examination of aramayoite, *Min. Mag.* **21**, 163–168.